Supplemental Data

Three Distinct Condensin Complexes

Control *C. elegans* Chromosome Dynamics

Gyorgyi Csankovszki, Karishma Collette, Karin Spahl, James Carey, Martha Snyder, Emily Petty, Uchita Patel, Tomoko Tabuchi, Hongbin Liu, Ian McLeod, James Thompson, Ali Sarkeshik, John Yates, Barbara Meyer, and Kirsten Hagstrom

SUPPLEMENTAL EXPERIMENTAL PROCEDURES

C. elegans strains

Animals were maintained on NG agar plates using standard methods. The following strains were used:

TY2386	wild type (N2)
TY4550	*capg-1(tm1514)* I/hT2 [qIs48] (I;III)
	capg-2 (tm1833) /nT1 [qIs51] (III;IV)
VC768	*kle-2 (ok1151)* III/ hT2 [qIs48] (I;III)
	kle-2 (tm1828) / hT2 [qIs48] (I;III)
	smc-4 (tm1868) III /qC1rol (III;V)
TY4341	*dpy-26(n199) unc-30(e191)* IV/nT1 [qIs51] (III;IV)
	dpy-26 (n199) IV /nT1 [qIs51] (III;IV)
	dpy-26 (n199) IV /nT1 [qIs51] (III;IV); hcp-6 (mr17) I
AR1	*hcp-6 (mr17)* I
TY3837	*dpy-28(s939)* III/qC1 III
TY148	*dpy-28(y1)* III
DR1410	*dpy-27 (y56)*/ qC1 *dpy-19* (e1259) *glp-1*(q339) III
TY1564	*unc-32(e189)dpy-27(y167)* III/qC1; *flu-2(e1008) xol-1(y9)* X
TY1072	*her-1(e1520)* V; *sdc-2(y74)* X
TY2205	*her-1(e1520) sdc-3(y126)* V; *xol-1(y9)* X
TY2384	*sex-1(y263)* X
TY4403	*him-8(e1489) IV; xol-1(y9) sex-1(y263) X*
AZ212	*unc-119 (ed3)* ruIs32[unc-119(+) pie-1::GFP::H2B] III.
PK125	*tra-2 (e2531)* II

Strains defective in dosage compensation

Dosage compensation mutations cause XX specific maternal effect lethality. *capg-1, dpy-26, dpy-28, dpy-27* null mutants were maintained as balanced strains. Homozygous mutants (animals lacking the balancer chromosomes) were picked individually from the population for staining experiments in Figure 5. *sdc-2* and *sdc-3* null mutants were maintained as XO animals in which the hermaphrodite mode of sex determination and dosage compensation had been switched on by a mutation in *xol-1*. The XO-specific lethality caused by the *xol-1*

mutation was suppressed by the *sdc-2* or *sdc-3* mutations. These strains have been used before to analyze localization in dosage compensation mutants [1-3].

Phylogenetic analysis

Phylogenetic analysis was performed using the maximum likelihood method ProtML from MOLPHY 2.3 [4], and alignments were done using T-COFFEE [5]. Alignments performed by MUSCLE [6] yielded similar results. Findings were also confirmed using PSI-BLAST analysis [7]. CAPG-1 protein sequence accession number is CAA98126, other accession numbers were obtained from [8].

RNAi assays to assess dosage compensation

The two RNAi assays used were described in [9].

Enhancement of lethality in the *sex-1(y263)* background: Wild type (control) and *sex-1(y263)* worms were grown on RNAi plates from L1 to adulthood. Three adults were moved to fresh RNAi plates and allowed to lay eggs for 24 hours. Hermaphrodite mothers were removed and total progeny counted. The next day, eggs not hatched were scored as dead progeny. % lethality was calculated as dead progeny/total progeny x100. At least 200 embryos were scored for each RNAi experiment.

Male rescue: *him-8(e1489); xol-1(y9) sex-1(y263)* hermaphrodites were grown from L1 to adulthood on RNAi plates. Two adults were moved to fresh plates and allowed to lay eggs for 24 hours. Total progeny was counted as soon as mothers were removed from the plates. In three days, progeny was scored as either male or hermaphrodite. Male rescue was calculated as # males/expected number of males x 100. The expected number of males was assumed to be 38% of total progeny, due to the presence of the *him-8* mutation [10]. At least 200 animals were scored for RNAi of each gene.

Assessing mitotic defects in XO hermaphrodites

To assess mitotic defects in hermaphrodites lacking dosage compensation (Figure 7B), wild-type males were crossed to hermaphrodites carrying a gain-of-function allele of the hermaphrodite-promoting sex determination gene *tra-2(e2531)* [11]. A short egg lay from the cross was made onto plates seeded with control and test RNAi feeding bacteria. 50% of the resulting progeny are XX hermaphrodites, and 50% are XO animals transformed to hermaphrodites by the *tra-2* mutation. These progeny were grown to adulthood, treated with Carnoy's fixative, stained with DAPI, and compared to wild-type XO males and XX hermaphrodites subjected to the same RNAi treatment and staining in parallel.

Antibodies

The following peptides were coupled to KLH and used for raising antibodies in rabbits (all proteins) and rats (CAPG-1):

DPY-27 (QPFKRRALTSDDDRPYADTDSMPEVDLDVDRRR)
KLE-2 (CFDDDEEDVRPRGERP)
CAPG-1 (PPKKRIRGPKLPALREEKSTGC)
CAPG-2 (CKNSLSSLLDVQLPDENRL)
DPY-26 (CKTTSDLGAIVEEEEMEE)
DPY-28 (CKSAVADDDSDSDEFMLDD)
Secondary antibodies were purchased from Jackson ImmunoResearch. Antibodies to SMC-4 [12], MIX-1 [13], DPY-26 [14], SDC-3 [15], and HCP-6 [16] have been described previously. In all cases, antibody staining patterns described were reduced or absent in the corresponding mutant or RNAi background. To identify mitotic cells, animals were co-stained with anti-alpha-tubulin antiserum (clone DM1A, Sigma).

Image collection
Images in Figures 3 (except bottom row), S3A&B (except top rows), S5A&B, 6A, and 7C&E were captured by a Hamamatsu ORCA–ER CCD camera using a Perkin Elmer UltraView RS-3 spinning disk confocal with a Zeiss Axiovert 200 microscope and a 100x objective. Of these, Figures S3B, 6A, S5A&B, 7C&E are projections of optical sections taken with a Z spacing of 0.4 microns; others are a single confocal plane. Images in Figures 6B, S5C, 7A, and S8 are wide-field fluorescence images captured by an ORCA-ER CCD camera mounted on a Leica DMIRE2 microscope. Images in Figures 3 (bottom row), 4, 5, 7D, S3A (top row), S3B (top row), S4 and S7 were captured with a Hamamatsu ORCA-ERGA CCD camera mounted on an Olympus BX61 motorized Z-drive microscope using a 100X oil immersion objective. Captured images were deconvolved using 3i Slidebook imaging software constrained iterative deconvolution algorithm. These images are projections of optical sections with a Z spacing of 0.3 micron.

Analysis of interacting proteins by MudPIT
Sample Preparation
To collect embryos, worms were grown to high density on egg plates [17]. Embryo extracts were prepared by sonicating in homogenization buffer (50mM HEPES-KOH pH7.6, 140 mM KCl, 1mM EDTA, 0.5% NP-40, 10% glycerol) with protease inhibitor cocktail, and the supernatant was collected after centrifugation at 5,000 x g for 20'. For large-scale IPs, 100 mg of total protein extract and 500 ug of antibody were used. Immunocomplexes were pulled down using 500 ul protein A sepharose beads and washed extensively (3 times in homogenization buffer, 3 times in homogenization buffer without glycerol or detergent), and eluted in 100 mM glycine (pH 2.5). TCA precipitated pellets were analyzed by MudPIT mass spectrometry (see below) [18].
To each of the four samples (which were all TCA precipitated protein pellets) 60 µL of 8 M Urea, 100 mM Tris, pH 8.5 were added to solubilize the protein. The subsequent mixture was then reduced by adding 0.3 µL of 1M TCEP (for a final concentration of 5 mM TCEP) and incubated at room temperature. To alkylate, 1.2 µL of Iodoacetamide (10 mM final concentration) were added and the samples were subsequently incubated at room temperature while in the dark for

15 minutes. Endoproteinase Lys-C (0.1 µg/µL) was then added in the amount of 1.0 µL and shaken for 4 hours while incubated in the dark at 37 ºC. The addition of 180 µL of 100 mM Tris pH 8.5 diluted the solutions to 2 M Urea. Calcium chloride (100 mM) was then added (2.4 µL) for a final concentration of 1 mM $CaCl_2$. Trypsin (0.5 µg/µL) was added in the amount of 4.0 µL. The resulting mixtures were then shaken for 18 hours and incubated in the dark at 37 ºC. To neutralize 15.00 µL of Formic Acid (90%) was added for a final concentration of 5% Formic Acid. The tubes were centrifuged for 30 minutes at 2 ºC on a table top centrifuge.

Multidimensional Protein Identification Technology (MudPIT):
Upon completion of the digestion, the proteins were pressure-loaded onto a fused silica capillary desalting column containing 3 cm of 5-µm strong cation exchange (SCX) followed by 3 cm of 5-µm C18 (reverse phase or RP material) packed into a undeactivated 250-µm i.d capillary. Using 1.5 mL of buffer A (95% water, 5% acetonitrile, and 0.1% formic acid) the desalting columns were washed overnight. Following the desalting process, a 100-µm i.d capillary consisting of a 10-µm laser pulled tip packed with 10 cm 3-µm Aqua C18 material (Phenomenex, Ventura, CA) was attached to the filter union (desalting column–filter union–analytical column). The resulting split-columns were placed inline with a ThermoFinnigan Surveyor MS Pump (Version 2.3; Palo Alto, CA) and analyzed using a customized 4-step separation method (90, 110, 110, and 150 minutes respectively).

Step 1 utilized only buffer A (95% water, 5% acetonitrile, and 0.1% formic acid) and buffer B (80% acetonitrile, 20% water, and 0.1% formic acid). It began with 5 min of 100% Buffer A, followed by the following buffer B gradients: 5 min of 0-10%, 40 min of 10-45%, and 10 min of 45-100%. Twenty minutes of 100% buffer B ensued and the gradient program ended with 10 min of 100% buffer A. Steps 2-4 utilized Buffers A, B, and C (500 mM ammonium acetate, 5% acetonitrile, and 0.1% formic acid). Steps 2 and 3 each began with: 3 min of 100% buffer A, 7 min of X% buffer C, a 5 min gradient from 0 – 10% buffer B, a 75 min gradient from 10-45% buffer B, and then 5 min of a 45-100% buffer B gradient. Five minutes of 100% buffer B followed and then the sequence ended with 10 min of 100% buffer A. The buffer C portions consisted of 20% for step 2 and 50% for step 3.

Step 4 began in a similar fashion (3 min of 100% buffer A, 7 min of 100% buffer C, and a 5 min gradient from 0 – 10% buffer B) yet its 10-45% buffer B gradient lasted for 85 minutes and the 45-100% buffer B gradient was for 10 min. Ten minutes of 100% and then a gradient of 0-100% buffer B ensued with the run ending with 10 min of 100% buffer A.

By increasing the salt concentration (buffer C) peptides “bump” off of the SCX and then with a gradient of increasing hydrophobicity (buffer B) the peptides can

elute from the RP into the ion source. To elute the peptides from the micro capillary column, a distal 2.5 kV spray voltage was applied. The applied voltage caused the peptides to directly electro spray into an LTQ 2-dimensional ion trap mass spectrometer (ThermoFinnigan, Palo Alto, CA). First a cycle of one full-scan mass spectrum (400-2000 m/z) and then 5 data-dependent MS/MS spectra at a 35% normalized collision energy was performed throughout each step of the multidimensional separation. The aforementioned HPLC solvent gradients and MS functions were all controlled by the Xcalibur data system (Version 1.4).

Analysis of Tandem Mass Spectra: As each step was executed, its spectra were recorded to a RAW file. This data was then converted into .ms2 format through the use of RawXtract (Version 1.9). From the .ms2 files, poor quality tandem mass spectra were removed using an automated spectral quality assessment algorithm known as a "PARC" filter [19]. The remaining MS/MS spectra were searched with the SEQUEST™ algorithm [20] against the WormBase_C-elegans protein database (created on 12/17/06). So as to assess the false positive rate the protein sequences from the database were reversed (decoy database) [21]. The number and quality of spectral matches to the decoy database were used to estimate the false positive rates. A computer cluster consisting of 100 1.2 GHz Athlon CPUs was used to perform the search [22]. The SEQUEST search did not employ any enzyme specifity and the final data set was filtered using the DTASelect™ (version 2.0.9) program [23, 24]. The digestion method employed was specified (--trypstat for tryptic digests) so as to specifically filter for peptides with trypsin specificity. A user-specified false positive rate was used to dynamically set XCorr and DeltaCN thresholds through quadratic discriminant analysis. This dataset was then further filtered to remove contaminants (i.e. keratin) while the default filter (minimum of 2 peptide and half tryptic status) was applied. Interacting proteins were ranked by estimated relative abundance using the total number of spectra observed for each [25].

SUPPLEMENTAL REFERENCES

1. Chuang, P.T., Albertson, D.G., and Meyer, B.J. (1994). DPY-27:a chromosome condensation protein homolog that regulates *C. elegans* dosage compensation through association with the X chromosome. Cell *79*, 459-474.
2. Chuang, P.T., Lieb, J.D., and Meyer, B.J. (1996). Sex-specific assembly of a dosage compensation complex on the nematode X chromosome. Science *274*, 1736-1739.
3. Yonker, S.A., and Meyer, B.J. (2003). Recruitment of *C. elegans* dosage compensation proteins for gene-specific versus chromosome-wide repression. Development *130*, 6519-6532.
4. Adachi, J., and Hasegawa, M. (1996). MOLPHY version 2.3: programs for molecular phylogenetics based on maximum likelihood. Comput. Sci. Monogr. *28*, 1-150.

5. Notredame, C., Higgins, D.G., and Heringa, J. (2000). T-Coffee: A novel method for fast and accurate multiple sequence alignment. J Mol Biol *302*, 205-217.
6. Edgar, R.C. (2004). MUSCLE: multiple sequence alignment with high accuracy and high throughput. Nucleic Acids Res *32*, 1792-1797.
7. Altschul, S.F., Madden, T.L., Schaffer, A.A., Zhang, J., Zhang, Z., Miller, W., and Lipman, D.J. (1997). Gapped BLAST and PSI-BLAST: a new generation of protein database search programs. Nucleic Acids Res *25*, 3389-3402.
8. Ono, T., Losada, A., Hirano, M., Myers, M.P., Neuwald, A.F., and Hirano, T. (2003). Differential contributions of condensin I and condensin II to mitotic chromosome architecture in vertebrate cells. Cell *115*, 109-121.
9. Gladden, J.M., Farboud, B., and Meyer, B.J. (2007). Revisiting the X:A signal that specifies *Caenorhabditis elegans* sexual fate. Genetics *177*, 1639-1654.
10. Phillips, C.M., Wong, C., Bhalla, N., Carlton, P.M., Weiser, P., Meneely, P.M., and Dernburg, A.F. (2005). HIM-8 binds to the X chromosome pairing center and mediates chromosome-specific meiotic synapsis. Cell *123*, 1051-1063.
11. Kuwabara, P.E. (1996). A novel regulatory mutation in the *C. elegans* sex determination gene *tra-2* defines a candidate ligand/receptor interaction site. Development *122*, 2089-2098.
12. Hagstrom, K.A., Holmes, V.F., Cozzarelli, N.R., and Meyer, B.J. (2002). *C. elegans* condensin promotes mitotic chromosome architecture, centromere organization, and sister chromatid segregation during mitosis and meiosis. Genes Dev *16*, 729-742.
13. Lieb, J.D., Albrecht, M.R., Chuang, P.T., and Meyer, B.J. (1998). MIX-1: an essential component of the *C. elegans* mitotic machinery executes X chromosome dosage compensation. Cell *92*, 265-277.
14. Lieb, J.D., Capowski, E.E., Meneely, P., and Meyer, B.J. (1996). DPY-26, a link between dosage compensation and meiotic chromosome segregation in the nematode. Science *274*, 1732-1736.
15. Davis, T.L., and Meyer, B.J. (1997). SDC-3 coordinates the assembly of a dosage compensation complex on the nematode X chromosome. Development *124*, 1019-1031.
16. Chan, R.C., Severson, A.F., and Meyer, B.J. (2004). Condensin restructures chromosomes in preparation for meiotic divisions. J Cell Biol *167*, 613-625.
17. Chu, D.S., Liu, H., Nix, P., Wu, T.F., Ralston, E.J., Yates, J.R., 3rd, and Meyer, B.J. (2006). Sperm chromatin proteomics identifies evolutionarily conserved fertility factors. Nature *443*, 101-105.
18. Delahunty, C.M., and Yates, J.R., 3rd (2007). MudPIT: multidimensional protein identification technology. Biotechniques *43*, 563, 565, 567 passim.
19. Bern, M., Goldberg, D., McDonald, W.H., and Yates, J.R., 3rd (2004). Automatic quality assessment of peptide tandem mass spectra. Bioinformatics *20 Suppl 1*, i49-54.

20. Eng, J., McCormack, A., and Yates, J.R., 3rd (1994). An Approach to Correlate Tandem Mass Spectral Data of Peptides with Amino Acid Sequences in a Protein Database. J Am Soc Mass Spectrom *5*, 976-989.
21. Peng, J., Elias, J.E., Thoreen, C.C., Licklider, L.J., and Gygi, S.P. (2003). Evaluation of multidimensional chromatography coupled with tandem mass spectrometry (LC/LC-MS/MS) for large-scale protein analysis: the yeast proteome. J Proteome Res *2*, 43-50.
22. Sadygov, R.G., Eng, J., Durr, E., Saraf, A., McDonald, H., MacCoss, M.J., and Yates, J.R., 3rd (2002). Code developments to improve the efficiency of automated MS/MS spectra interpretation. J Proteome Res *1*, 211-215.
23. Cociorva, D., D, L.T., and Yates, J.R. (2007). Validation of tandem mass spectrometry database search results using DTASelect. Curr Protoc Bioinformatics *Chapter 13*, Unit 13 14.
24. Tabb, D.L., McDonald, W.H., and Yates, J.R., 3rd (2002). DTASelect and Contrast: tools for assembling and comparing protein identifications from shotgun proteomics. J Proteome Res *1*, 21-26.
25. Liu, H., Sadygov, R.G., and Yates, J.R., 3rd (2004). A model for random sampling and estimation of relative protein abundance in shotgun proteomics. Anal Chem *76*, 4193-4201.

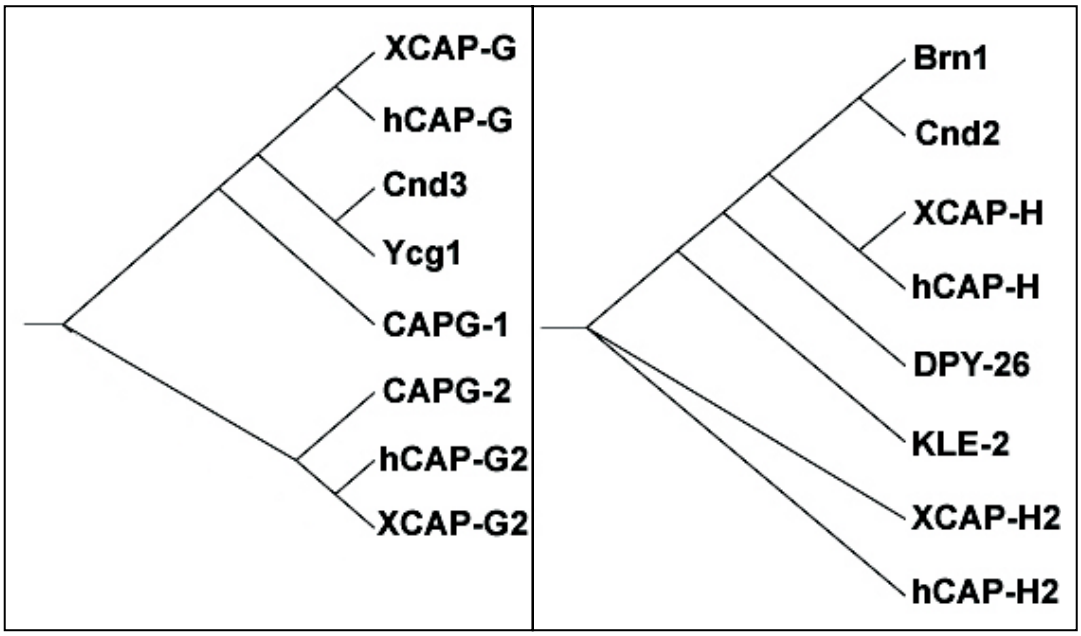

Figure S1. Phylogenetic analysis of CAP-G/G2 and CAPH/H2 subunits.
C. elegans CAPG-1 is more closely related to CAP-G proteins, while CAPG-2 is more closely related to CAP-G2 proteins. Similarly, while DPY-26 is related to CAP-H proteins, KLE-2 is more closely related to CAP-H2 proteins. Phylogenetic analysis of CAP-D2/D3 proteins was reported in Chan et al., 2004. Together these analyses show that the CAP subunits of *C. elegans* condensin I^{DC} and condensin I belong to the CAP I class, and the CAP subunits of condensin II belong to the CAP II class.

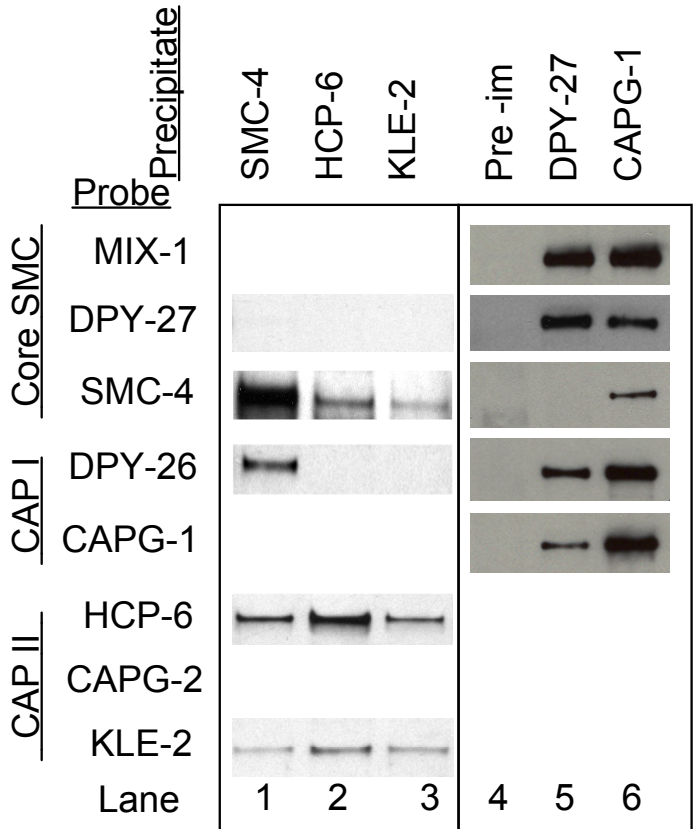

Figure S2. Condensin subunit interactions analyzed by immunoprecipitation and Western blotting.
Images of selected Western blots which confirm the results obtained by mass spectrometry. Immunoprecipitation (IP) reactions from embryo extracts using antibodies against condensin subunits were performed, listed at the top. Each IP was analyzed on Western blots probed with an array of antibodies, listed on the left.

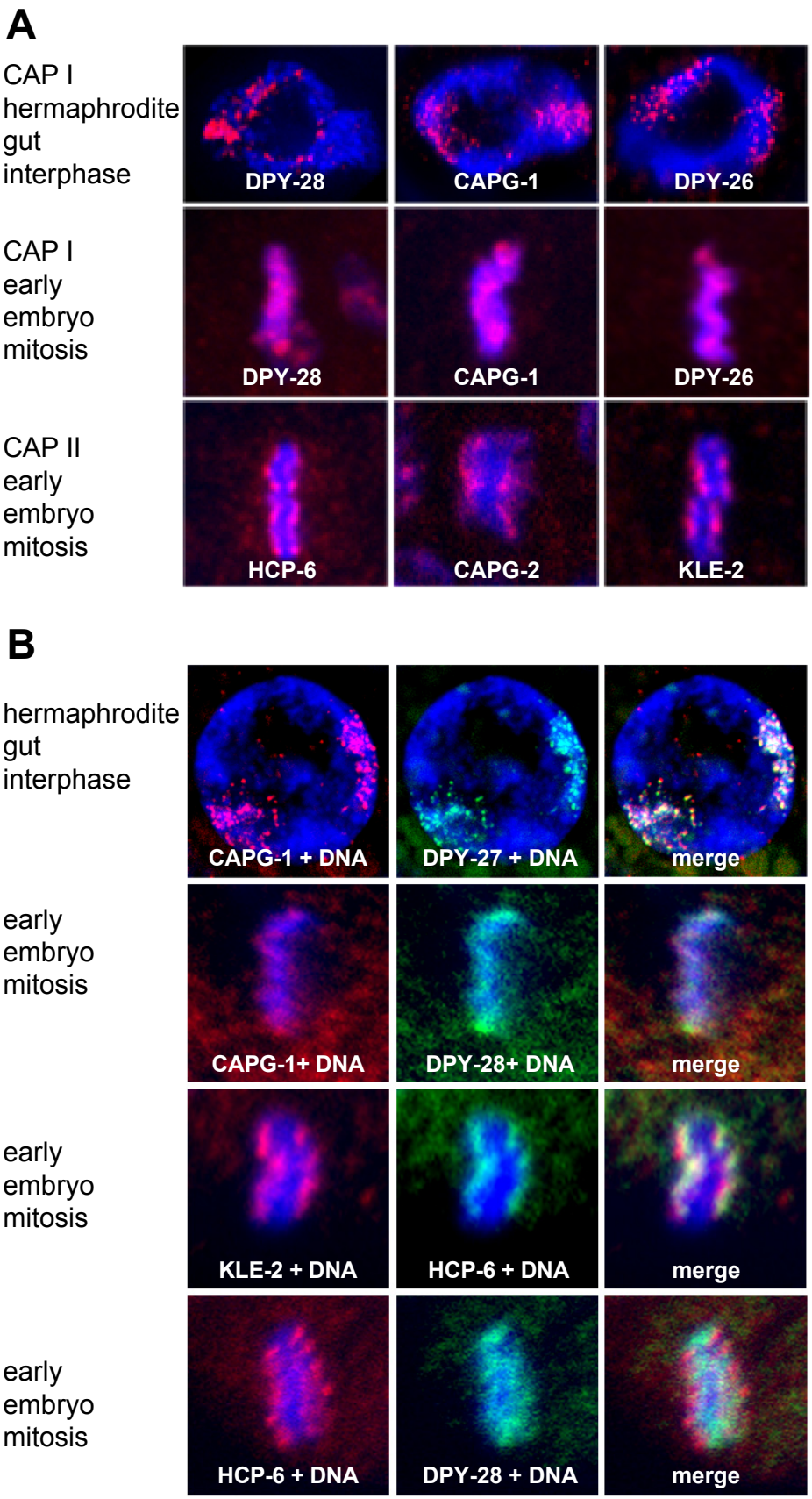
A
CAP I hermaphrodite gut interphase
DPY-28
CAPG-1
DPY-26
CAP I early embryo mitosis
DPY-28
CAPG-1
DPY-26
CAP II early embryo mitosis
HCP-6
CAPG-2
KLE-2
B
hermaphrodite gut interphase
CAPG-1 + DNA
DPY-27 + DNA
merge
early embryo mitosis
CAPG-1+ DNA
DPY-28+ DNA
merge
early embryo mitosis
KLE-2 + DNA
HCP-6 + DNA
merge
early embryo mitosis
HCP-6 + DNA
DPY-28 + DNA
merge

Figure S3. Newly identified subunits co-localize with known subunits, but condensin I and condensin II do not co-localize.
(A) All three CAP subunits of each class show the same localization patterns. The three class I CAP subunits (DPY-28, CAPG-1, and DPY-26) associate with hermaphrodite interphase nuclei in the sub-regions occupied by the X chromosomes (top row) and coat mitotic chromosomes at the metaphase plate of early embryos (middle row). The three class II subunits (HCP-6, CAPG-2, and KLE-2) all show similar centromere-enriched pattern on mitotic chromosomes at the metaphase plate (bottom row). Antibody in red, DNA in blue, merge in pink. **(B)** CAPG-1 (red) colocalizes with condensin I^{DC} subunit DPY-27 (green) on X chromosomes of interphase intestinal nuclei of hermaphrodites and with condensin I subunit DPY-28 on mitotic chromosomes of early embryos. KLE-2 (red) colocalizes with condensin II subunit HCP-6 (green) on the outer face of mitotic chromosomes of early embryos. Bottom row: Condensin II subunit HCP-6 (red) localizes to outer face of the metaphase plate, while condensin I subunit DPY-28 (green) associates non-uniformly with chromosomes in a diffuse manner, with minimal overlap between the two complexes. DNA in blue.

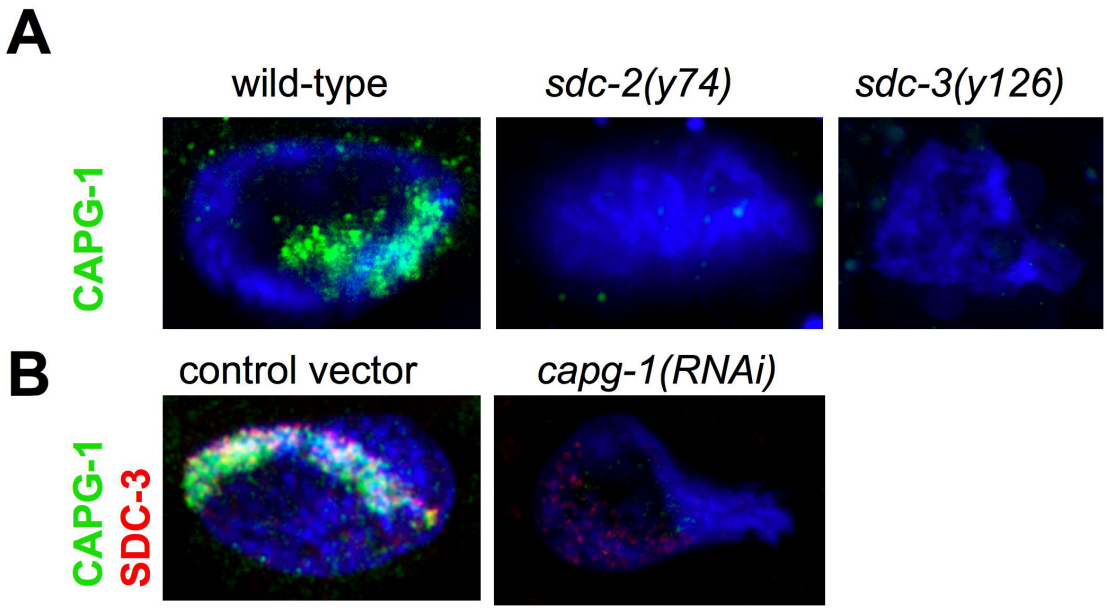

Figure S4. CAPG-1 shows X chromosome binding relationships with SDC proteins.

(A) CAPG-1 (green) localizes to hermaphrodite X chromosomes in wild type animals, but not in animals carrying mutations in *sdc-2* or *sdc-3*, genes required for both sex-determination and dosage compensation. **(B)** *capg-1* RNAi does not eliminate, but greatly reduces, staining by SDC-3 specific antibodies (red). DNA in blue.

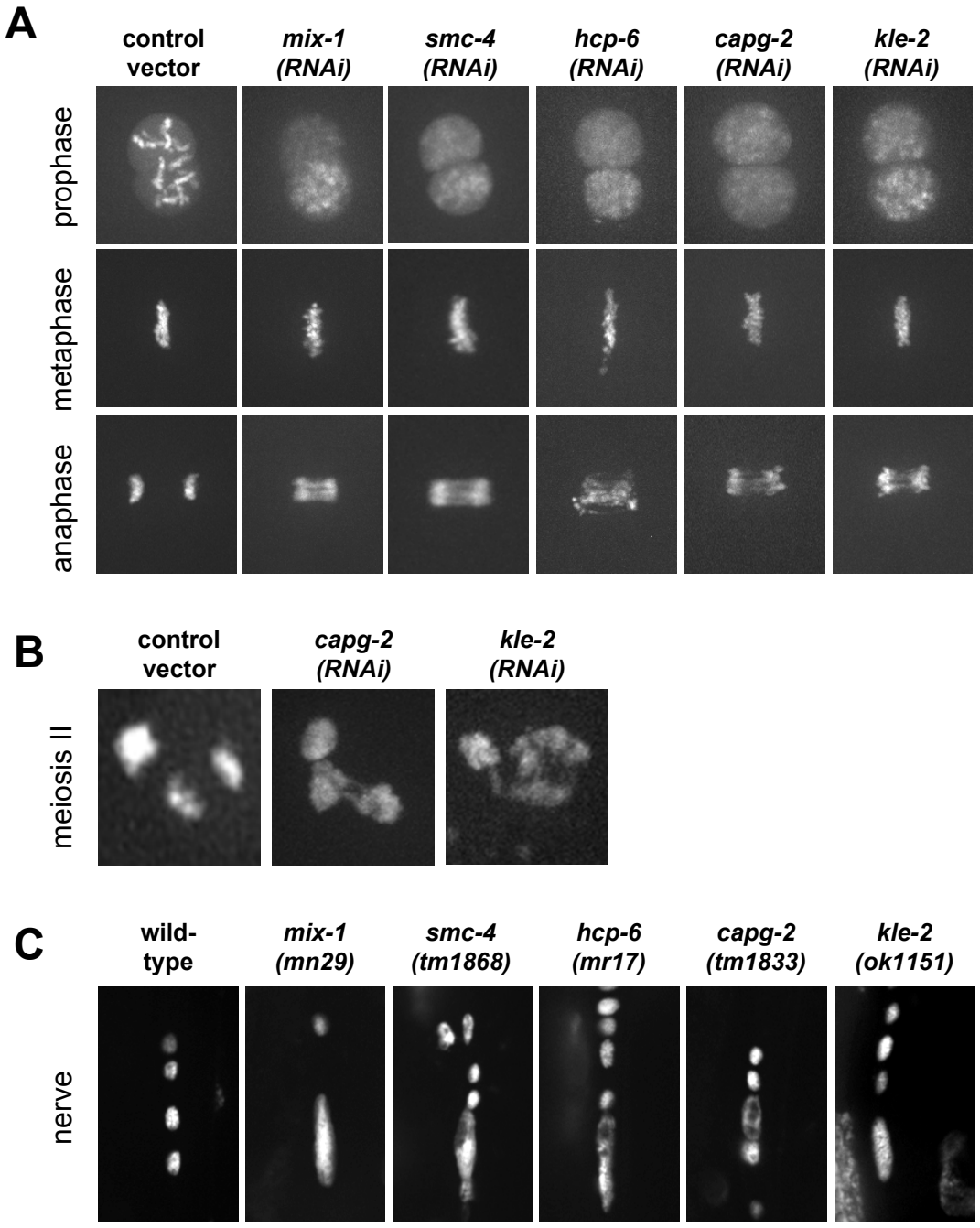

Figure S5. Common chromosomal and developmental defects result from depletion of each condensin II subunit.

(A) Three frames from time-lapse movies of the first embryonic mitosis in a strain carrying GFP:histone H2B to visualize chromosomes. RNAi-mediated depletion of each condensin II subunit was achieved by combining dsRNA injection and RNAi feeding into the adult hermaphrodite parent. In control treated animals, condensation during prophase occurs normally and chromosomes adopt distinct rod shapes (top left). In contrast, identical disorganized chromosome morphology is observed after depleting each condensin II subunit

(top row). Chromosomes depleted of condensin II subunits condense to a fair degree by metaphase (middle row), but depletion of each subunit causes a similar failure in anaphase segregation and DNA bridges are apparent (bottom row). **(B)** Images from time-lapse movies of meiosis II in a GFP:histone H2B strain after two generations of RNAi feeding. In each panel the first polar body (one set of homologs from meiosis I) is visible at the top left, and segregating chromosomes at anaphase II are visible bottom right. In control treated animals the sets of chromosomes are completely separated (left). Depletion of either *capg-2* or *kle-2* leads to incompletely separated meiotic chromosomes, as previously reported for *hcp-6* depletion. **(C)** Nerve cell nuclei visualized by DAPI staining are uniformly sized and evenly spaced in wild-type. Mutant alleles of each condensin II subunit exhibit a common defect in which two or more of these nuclei appear fused, presumably from failed chromosome segregation in the prior mitosis.

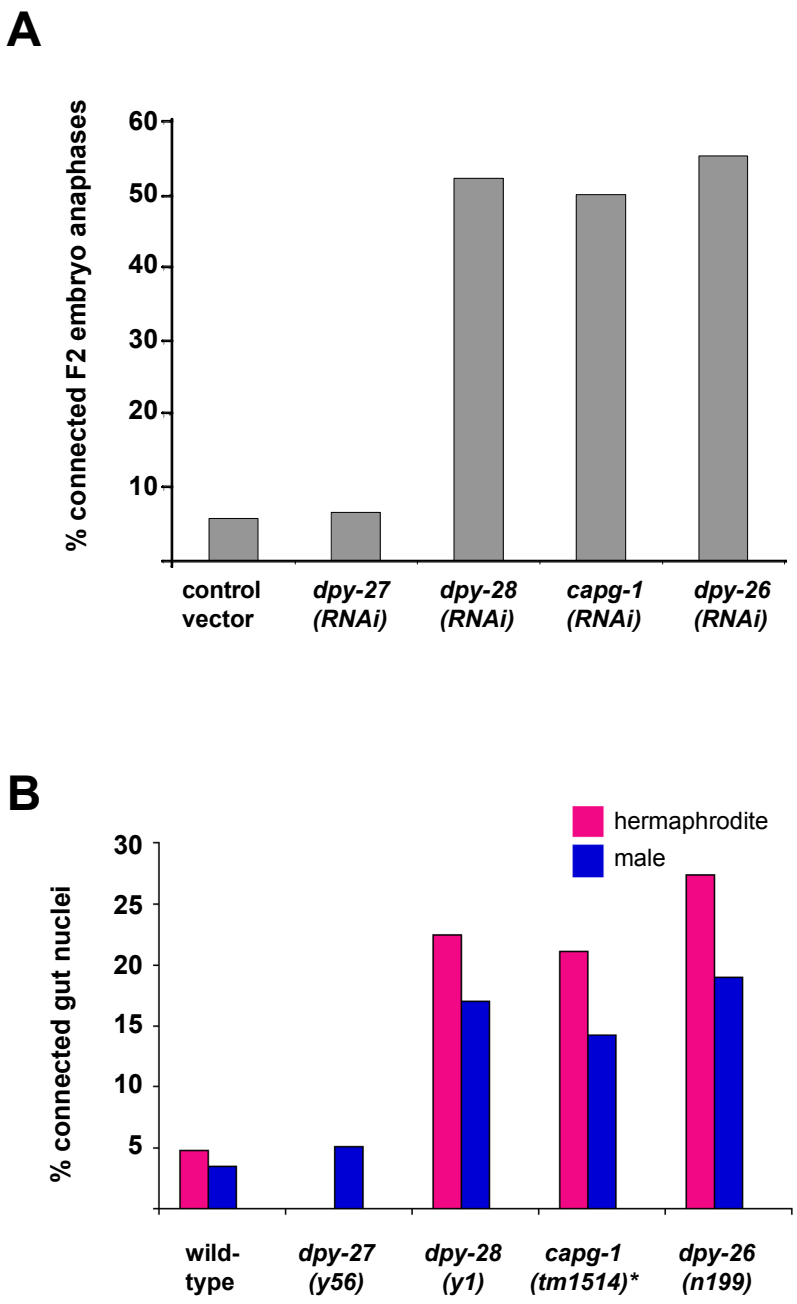

Figure S6. Mutational or RNAi-mediated depletion of class I CAP subunits, but not of *dpy-27*, shows chromosome separation defects.

(A) Two generations of RNAi feeding with control empty vector or dsRNA targeting *dpy-27, dpy-28, capg-1*, or *dpy-26* were performed in a strain carrying GFP:histone H2B and mitotic chromosomes were visualized in their early stage embryos. The percent of total anaphases in which chromosomes appeared connected by DNA bridges (see Figure 7C) were scored. Depletion of the condensin I^{DC} specific subunit *dpy-27* was not significantly different from control vector while *dpy-28*, *capg-1*, or *dpy-26* depletion showed a high percentage of

failed anaphases. **(B)** Wild-type and mutant adult hermaphrodites (magenta) and males (blue) were stained with DNA dye and scored for the percentage of connected gut nuclei. *capg-1(tm1514)* homozygotes were scored from heterozygous mothers, while all other strains were scored as homozygotes from homozygous mothers. This generation of *dpy-27(y56)* hermaphrodites do not live to adulthood so only males were scored, and showed a low percentage of connected gut nuclei as in wild-type. In contrast, a high percent of abnormally connected nuclei were observed in both sexes in strains carrying mutations in each class I CAP subunit. For all cases in both A and B, *dpy-27* depletion was not significantly different from vector or wild-type ($p>0.1$) while *dpy-28*, *capg-1*, or *dpy-26* depletion was significantly different ($p<0.0001$) by Fisher's exact test.

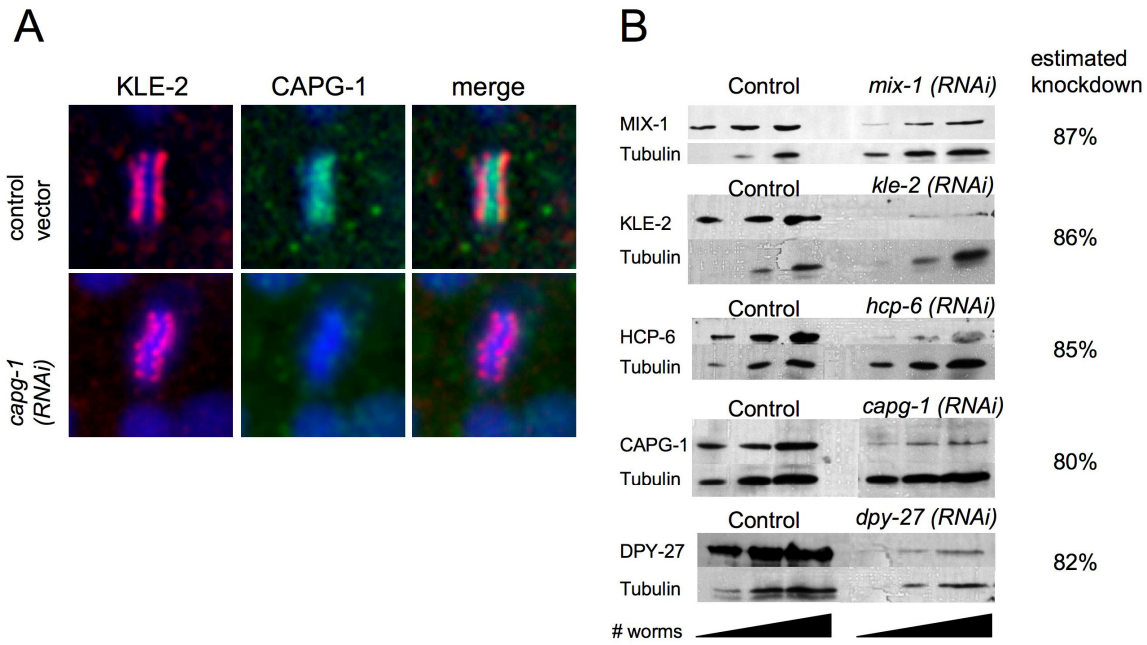

Figure S7. Condensin I depletion does not disrupt condensin II localization during mitosis, and RNAi feeding produces substantial but not complete depletion.

(A) Metaphase chromosomes from young F2 embryos after two generations of control vector RNAi or *capg-1* RNAi feeding. Embryos were stained with antibodies specific to KLE-2 and CAPG-1. After *capg-1* RNAi, CAPG-1 protein is below the level of detection by immunofluorescence, but KLE2 patterns (presumably reflecting condensin II localization) are unaltered.

(B) Western blot analysis of the extent of depletion in adults after one-generation (*mix-1, kle-2, hcp-6*) or two-generation (*capg-1, dpy-27*) feeding RNAi (see methods). Pixel intensity of the targeted subunit was quantified relative to a tubulin control for each of three different concentrations of loaded worms. Intensities were plotted, and a rough estimate of knockdown from the lane that appeared to be in a linear range is shown. Each subunit appears to be knocked down to a similar degree by RNAi feeding, with substantial but not complete depletion. Independent replicates of some subunit RNAi treatments were quantified and give roughly similar levels of knockdown (data not shown).

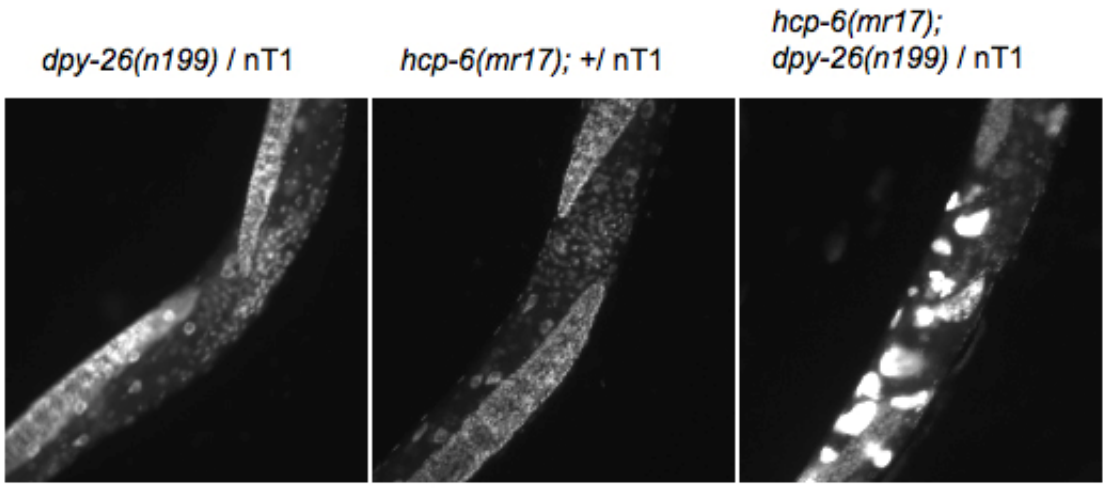

Figure S8. Double depletion of a class I and a class II CAP is more severe than either single depletion.
Adult hermaphrodites stained with DNA dye, showing the central body region between the two gonad arms. Animals heterozygous for the class I CAP allele *dpy-26(n199)* or homozygous for the class II CAP temperature-sensitive allele *hcp-6(mr17)* show normal nuclear appearance at the permissive temperature of 15^{o}. In contrast, animals carrying both mutations show severe defects in nuclear morphology at the permissive temperature. For example, double mutants have a greater proportion of connected gut nuclei than either single (data not shown), and in the germline produce what appear to be large, polyploid nuclei. These may represent endomitotic oocytes that underwent repeated rounds of DNA replication without division. Endomitotic oocytes can result from several types of defects, including a failure in meiosis or oocyte maturation. Such endomitotic oocytes are observed, but to a lesser extent, in homozygous *dpy-26(n199)* animals or those depleted of condensin I CAPs by two-generation RNAi feeding (data not shown). nT1 is a translocation chromosome used as a genetic balancer for the *dpy-26* allele and is present in each strain for consistency.